High-mass gamma-ray binaries as very efficient accelerators

Valentí Bosch-Ramon

Universitat de Barcelona, ICCUB, IEEC

Gamma 2022 Symposium Barcelona

July 7th, 2022

Outline

Outline

High-mass gamma-ray binaries (with CO)

- **The phenomenological term *Gamma-ray binary* usually means star+CO and SED dominance of gamma rays (without the star).**
- **High-mass gamma-ray binaries (HMGB) are among the most powerful galactic sources: $L \sim 10^{36-37}$ (MeV), 10^{34-37} (GeV) and 10^{32-35} erg s^{-1} (TeV).**
- **The great majority of the known HMGB are VHE emitters.**

(Some reviews: Mirabel 2006; Romero 2009; B-R & Khangulyan 2009; Dubus 2015; Paredes & Bordas 2019; Chernyakova & Malyshev 2020...)

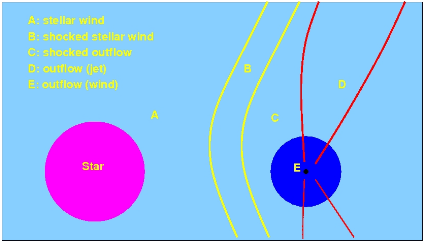

Main elements of a HMGB.

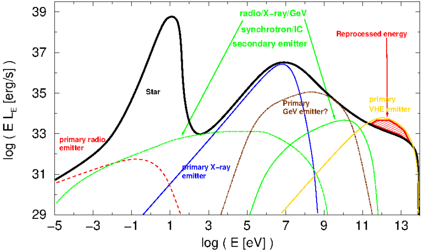

Typical SED of a HMGB.

- **The phenomenological term** *Gamma-ray binary* **usually means star+CO and SED dominance of gamma rays (without the star).**
- **High-mass gamma-ray binaries (HMGB) are among the most powerful galactic sources:** $L \sim 10^{36-37}$ **(MeV),** 10^{34-37} **(GeV) and** 10^{32-35} **erg** s^{-1} **(TeV).**
- **The great majority of the known HMGB are VHE emitters.**

(Some reviews: Mirabel 2006; Romero 2009; B-R & Khangulyan 2009; Dubus 2015; Paredes & Bordas 2019; Chernyakova & Malyshev 2020...)

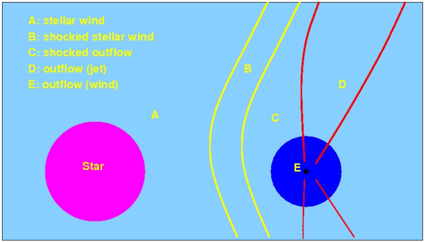

Main elements of a HMGB.

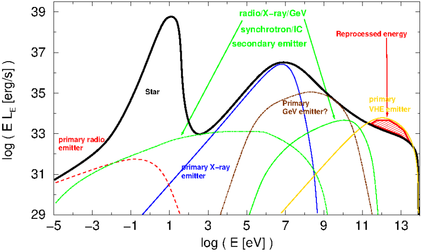

Typical SED of a HMGB.

High-mass gamma-ray binaries (with CO)

- **The phenomenological term *Gamma-ray binary* usually means star+CO and SED dominance of gamma rays (without the star).**
- **High-mass gamma-ray binaries (HMGB) are among the most powerful galactic sources: $L \sim 10^{36-37}$ (MeV), 10^{34-37} (GeV) and 10^{32-35} erg s^{-1} (TeV).**
- **The great majority of the known HMGB are VHE emitters.**

(Some reviews: Mirabel 2006; Romero 2009; B-R & Khangulyan 2009; Dubus 2015; Paredes & Bordas 2019; Chernyakova & Malyshev 2020...)

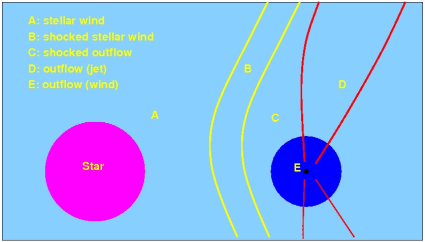

Main elements of a HMGB.

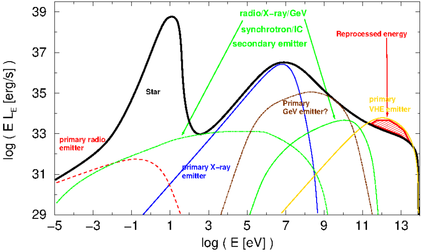

Typical SED of a HMGB.

Non-accreting (pulsar) vs accreting (HMMQ) HMGB

- **A non-accreting HMGB consists of a young pulsar plus an OB star whose winds interact.**
- A HMMQ consists of a CO plus an OB star in which the wind is accreted and jets form, which interact with the wind.
- In both cases, outflows interacting along the orbit are complex and emit radio, X- and gamma rays, likely through synchrotron and IC, plus $\gamma\gamma$...

(e.g., B-R, Khangulyan, Aharonian, Barkov, Perucho + ...; Bogovalov, + ...; Romero, + ...; Dubus, Lamberts, Cerutti + ...; Sierpowska-Bartosik, Torres, + ...; Bednarek, + ...; Reitberger, Reimer, Huber, Kissmann; Yoon, Heinz, + ...; Chernyakova, Neronov, + ...; Takata, Kong, Cheng, + ...; etc.)

(see e.g. Molina's talk -Wednesday- and Kefala's poster)

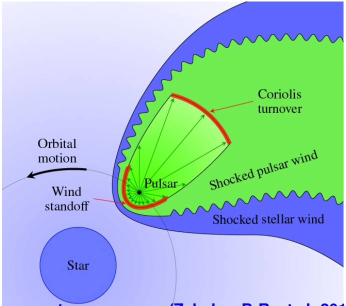

High-mass star+young psr (Zabalza, B-R, et al. 2013)

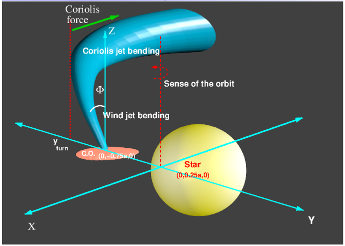

High-mass microquasar (Barkov & B-R 2021)

Non-accreting (pulsar) vs accreting (HMMQ) HMGB

- **A non-accreting HMGB consists of a young pulsar plus an OB star whose winds interact.**
- **A HMMQ consists of a CO plus an OB star in which the wind is accreted and jets form, which interact with the wind.**
- **In both cases, outflows interacting along the orbit are complex and emit radio, X- and gamma rays, likely through synchrotron and IC, plus $\gamma\gamma$...**

(e.g., B-R, Khangulyan, Aharonian, Barkov, Perucho + ...;

Bogovalov, + ...; Romero, + ...; Dubus, Lamberts, Cerutti + ...;

Sierpowska-Bartosik, Torres, + ...; Bednarek, + ...; Reitberger,

Reimer, Huber, Kissmann; Yoon, Heinz, + ...; Chernyakova,

Neronov, + ...; Takata, Kong, Cheng, + ...; etc.)

(see e.g. Molina's talk -Wednesday- and Kefala's poster)

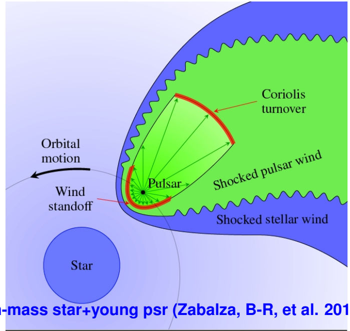

High-mass star+young psr (Zabalza, B-R, et al. 2013)

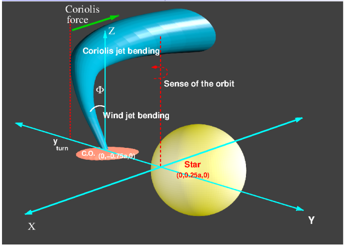

High-mass microquasar (Barkov & B-R 2021)

Non-accreting (pulsar) vs accreting (HMMQ) HMGB

- **A non-accreting HMGB consists of a young pulsar plus an OB star whose winds interact.**
- **A HMMQ consists of a CO plus an OB star in which the wind is accreted and jets form, which interact with the wind.**
- **In both cases, outflows interacting along the orbit are complex and emit radio, X- and gamma rays, likely through synchrotron and IC, plus $\gamma\gamma$...**

(e.g., B-R, Khangulyan, Aharonian, Barkov, Perucho + ...; Bogovalov, + ...; Romero, + ...; Dubus, Lamberts, Cerutti + ...; Sierpowska-Bartosik, Torres, + ...; Bednarek, + ...; Reitberger, Reimer, Huber, Kissmann; Yoon, Heinz, + ...; Chernyakova, Neronov, + ...; Takata, Kong, Cheng, + ...; etc.)

(see e.g. Molina's talk -Wednesday- and Kefala's poster)

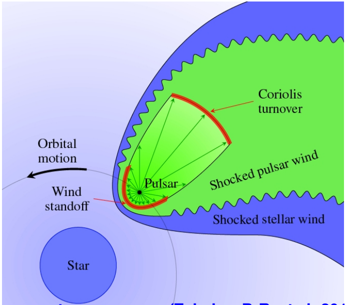

High-mass star+young psr (Zabalza, B-R, et al. 2013)

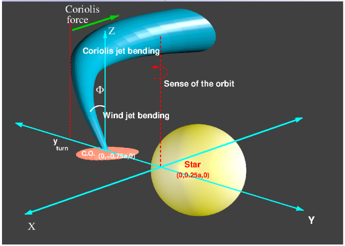

High-mass microquasar (Barkov & B-R 2021)

Non-accreting HMGB

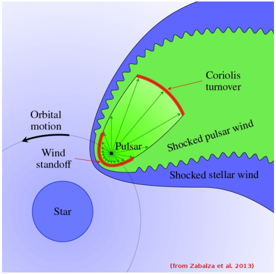

(Zabalza, B-R, et al. 2013)

RHD simulations with PLUTO of 2-wind-orbit interactions (low *e*).

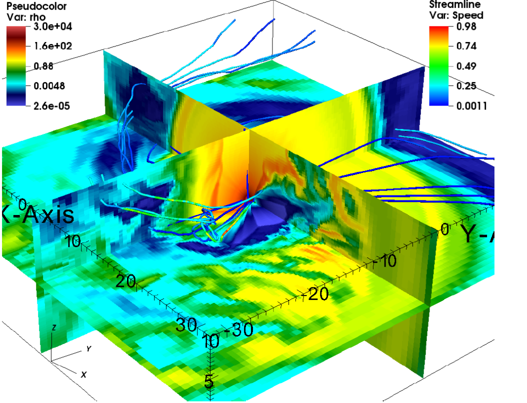

Fig. 2. Representation of the distribution of density in the XY-, XZ-, and YZ-planes for 3DIf at t = 3.9 days (apastron). Streamlines are shown in 3D.

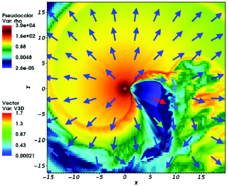

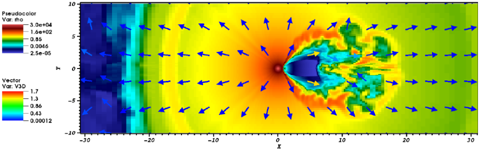

(LS 5039 at apastron; B-R, Barkov & Perucho 2015;see also Kissmann's talk from Wednesday)

High-mass microquasar

RHD simulations with PLUTO of jet-wind-orbit interactions.

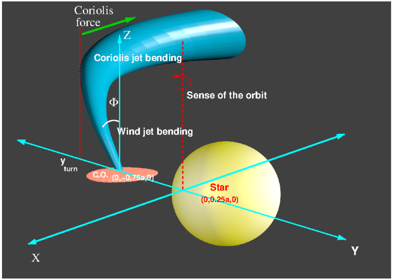

(HMMQ jet in a $e = 0$ orbit; Barkov & B-R 2021)

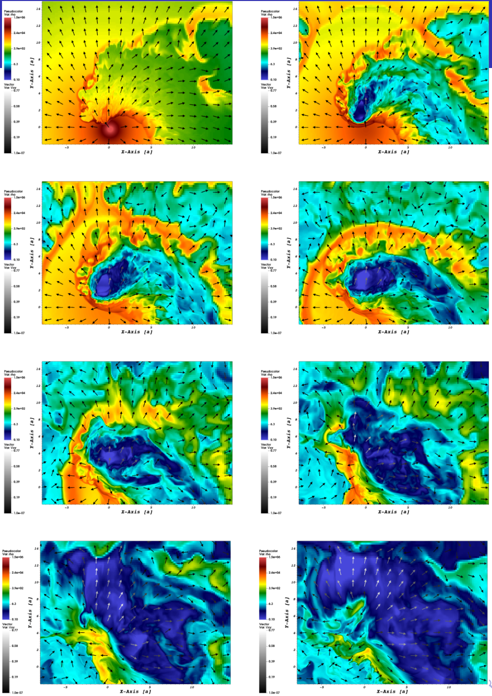

Outline

Eccentric, relatively compact Be+CO? binary (end of 70s)

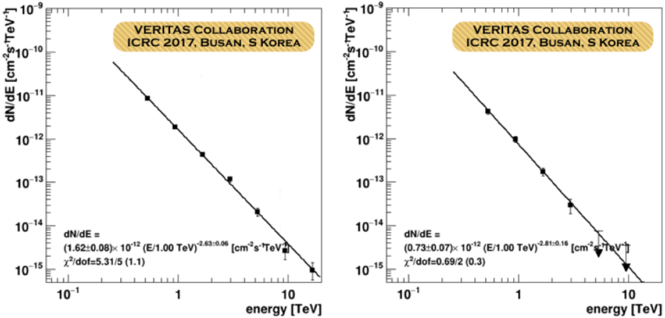

Figure 3: Spectral energy distribution (SED) for LS I +61°303 for two parts of the orbit (parts of the orbit shown on top panels). SED on the *left* is near apastron passage covering $\phi = 0.5 \rightarrow 0.8$ and SED on the *right* is for the rest of the orbit for $\phi = 0.8 \rightarrow 0.5$. The orbital parameters shown on top panel are used from [14]

(VERITAS: Kar et al. 2017)

VHE spectrum of PSR B1259−63

Highly eccentric, wide Be+pulsar binary (beginning of 90s)

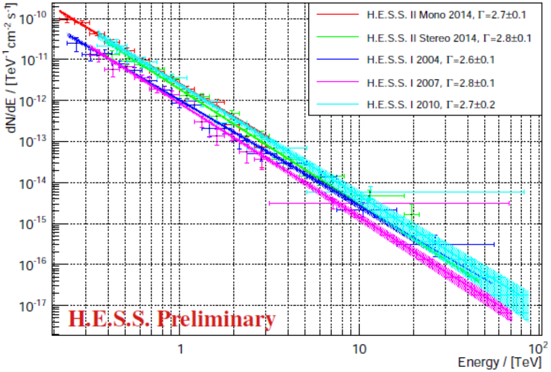

(HESS: Bordas et al. 2015)

VHE spectrum of LS 5039

Moderately eccentric, compact O+CO? binary (90s)

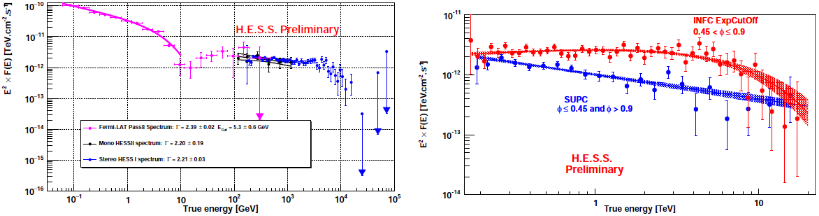

FIGURE 4. *Left*: SEDs obtained from monoscopic and a stereoscopic analyses of the H.E.S.S.-II and H.E.S.S.-I data sets, respectively. Results of fits with power-law functions are given in the inset. Also an SED obtained from a re-analysis of Fermi-LAT data is shown. *Right*: SEDs resulting from H.E.S.S.-I analyses for parts of the orbit corresponding to the inferior or superior conjunction. The corresponding orbital phase ranges are given for reference. Fit results are given in the main text.

(HESS: Bordas et al. 2015; also detected by HAWC)

VHE spectrum of HESS J0632+057

Eccentric, rather wide Be+CO? binary (00s)

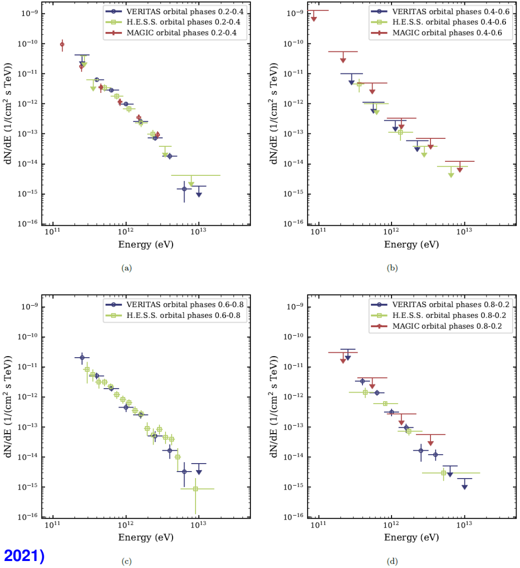

(HESS, MAGIC & VERITAS 2021)

Figure 7. Differential energy spectra of photons above 200 GeV obtained by H.E.S.S., MAGIC and VERITAS averaged over all available orbits. The figure shows the results for four different orbital phase bins: (a) orbital phases 0.2–0.4; (b) orbital phases 0.4–0.6; (c) orbital phases 0.6–0.8; (d) orbital phases 0.8–0.2. Vertical error bars show 1σ uncertainties; downwards pointing arrows indicate upper limits at the 95% confidence level.

Moderately eccentric?, relatively compact O+CO? binary (10s)

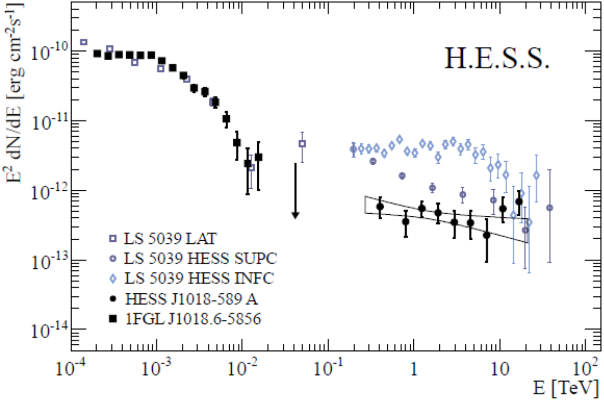

(HESS 2015)

Fig. 1. SED of HESS J1018–589 A/1FGL J1018.6–5856 is shown in black (filled squares and circles for the LAT and HESS detection). For comparison, the SEDs of LS 5039 during superior (SUPC) and inferior conjunction (INFC) are also included (blue points from Hadasch et al. 2012; Aharonian et al. 2005a).

VHE spectrum of PSR J2032+4127

Extremely eccentric, very wide Be+pulsar binary (00s or 10s?)

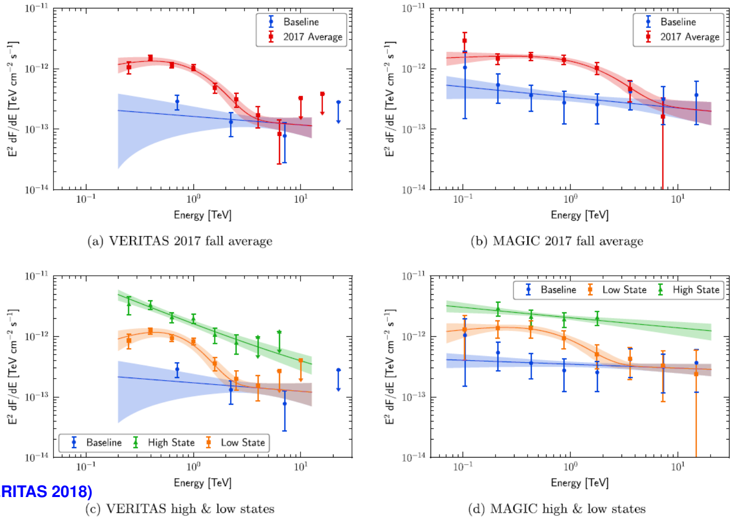

(a) VERITAS 2017 fall average

(b) MAGIC 2017 fall average

(c) VERITAS high & low states

(d) MAGIC high & low states

(MAGIC, VERITAS 2018)

Figure 3. Spectral energy distributions for PSR J2032+4127/MT91 213 and TeV J2032+4130 from VERITAS (left) and MAGIC (right). The blue butterflies are the spectral fits to TeV J2032+4130. The red butterflies in the upper plots are fits to the 2017 fall data: the sum of a power-law fit to TeV J2032+4130 and a cutoff power-law fit to PSR J2032+4127/MT91 213. In the bottom plots, orange is the fit to the low-state data (PSR J2032+4127/MT91 213 is fit with a cutoff), while green represents the high-state data (PSR J2032+4127/MT91 213 is fit with a power law). The fit parameters are given in Table 1 and the time periods are defined in the text.

VHE spectrum of LMC P3

Moderately eccentric, compact O+CO? binary (10s)

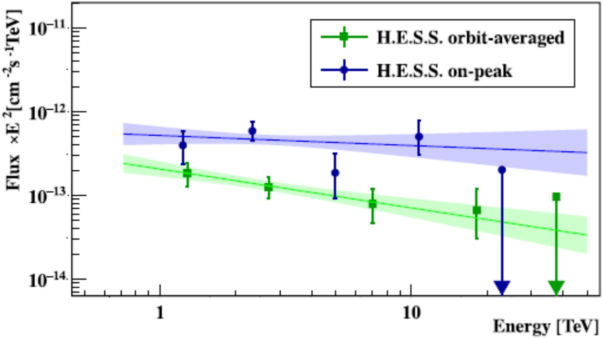

(HESS 2018)

Fig. 3. Spectral energy distribution averaged over the full orbit (green, squares) and for the on-peak orbital phase range (orbital phase from 0.2 to 0.4: blue, circles). The data points have 1 σ statistical error bars, upper limits are for a 95% confidence level. The best fit and its uncertainty are represented by the solid lines and shaded areas, respectively.

4FGL J1405.1-6119

- **The source is rather similar to LS 5039 and 1FGL J1018.6−5856.**
- **It is not known so far if this source emits VHE.**
- **The HE spectral information does not allow extrapolation.**

(see Corbet et al. 2019)

4FGL J1405.1-6119

- **The source is rather similar to LS 5039 and 1FGL J1018.6−5856.**
- **It is not known so far if this source emits VHE.**
- **The HE spectral information does not allow extrapolation.**

(see Corbet et al. 2019)

4FGL J1405.1-6119

- **The source is rather similar to LS 5039 and 1FGL J1018.6−5856.**
- **It is not known so far if this source emits VHE.**
- **The HE spectral information does not allow extrapolation.**

(see Corbet et al. 2019)

VHE spectrum of HESS J1832−093

Moderately wide O?+CO? binary? (10s)

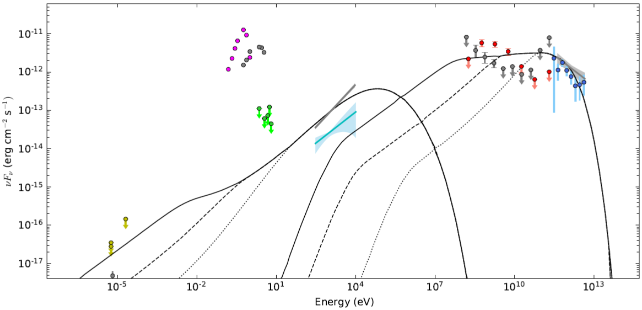

(Martí-Devesa & Reimer 2020 ↑, Tam et al. 2019, and ref. therein; HESS 2015, Eger et al. 2016)

Outline

Acceleration sites

- **Plenty of potential accelerators (via Fermi I, II and shear; *B*-reconnect.; converter mech.).**
- **Ultrarelativistic weak-B' flow.**
- **Perpendicular/oblique shocks of different speeds and strength (B'?).**
- **Flow reacceleration and further shocks, shear layers, turbulence and mass-loading... (B'?)**

(e.g., Rieger et al. 2007; Khangulyan et al. 2008; B-R & Khangulyan 2009; Takahashi et al. 2009 B-R 2012; B-R & Rieger 2012, Derishev & Aharonian 2012)

(B-R et al. 2012 -2D-, 2015 -3D-; low *e*)→

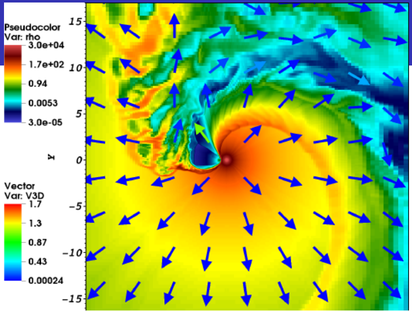

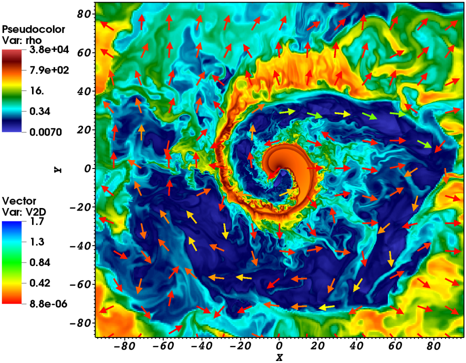

Acceleration sites

- **Plenty of potential accelerators (via Fermi I, II and shear; *B*-reconnect.; converter mech.).**
- **Ultrarelativistic weak-B' flow.**
- **Perpendicular/oblique shocks of different speeds and strength (B'?).**
- **Flow reacceleration and further shocks, shear layers, turbulence and mass-loading... (B'?)**

(e.g., Rieger et al. 2007; Khangulyan et al. 2008; B-R & Khangulyan 2009; Takahashi et al. 2009 B-R 2012; B-R & Rieger 2012, Derishev & Aharonian 2012)

(B-R et al. 2012 -2D-, 2015 -3D-; low *e*)→

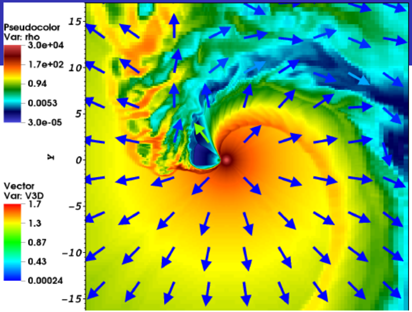

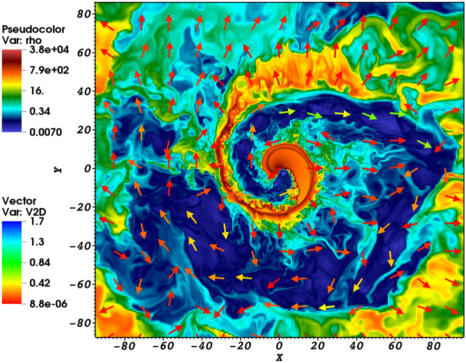

Acceleration sites

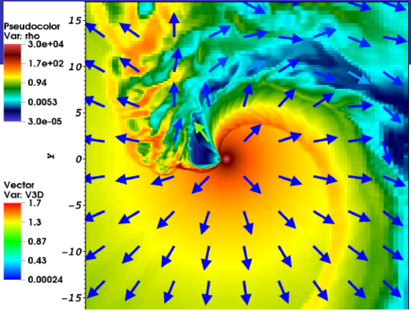

- **Plenty of potential accelerators (via Fermi I, II and shear; *B*-reconnect.; converter mech.).**
- **Ultrarelativistic weak-B' flow.**
- **Perpendicular/oblique shocks of different speeds and strength (B'?).**
- **Flow reacceleration and further shocks, shear layers, turbulence and mass-loading... (B'?)**

(e.g., Rieger et al. 2007; Khangulyan et al. 2008; B-R & Khangulyan 2009; Takahashi et al. 2009 B-R 2012; B-R & Rieger 2012, Derishev & Aharonian 2012)

(B-R et al. 2012 -2D-, 2015 -3D-; low *e*)$\rightarrow$

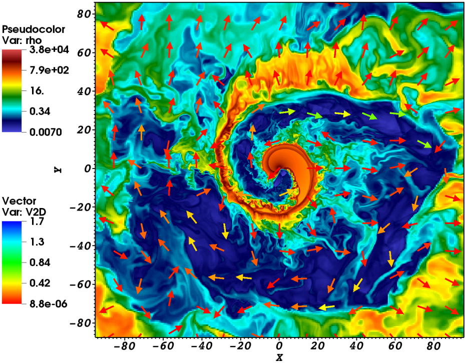

Acceleration sites

- **Plenty of potential accelerators (via Fermi I, II and shear; *B*-reconnect.; converter mech.).**
- **Ultrarelativistic weak-B' flow.**
- **Perpendicular/oblique shocks of different speeds and strength (B'?).**
- **Flow reacceleration and further shocks, shear layers, turbulence and mass-loading... (B'?)**

(e.g., Rieger et al. 2007; Khangulyan et al. 2008; B-R & Khangulyan 2009; Takahashi et al. 2009 B-R 2012; B-R & Rieger 2012, Derishev & Aharonian 2012)

(B-R et al. 2012 -2D-, 2015 -3D-; low *e*)→

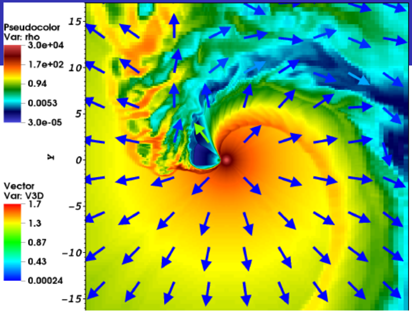

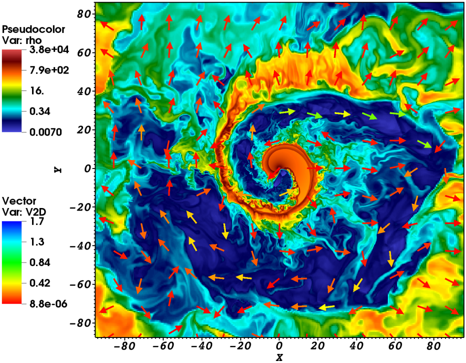

Acceleration sites

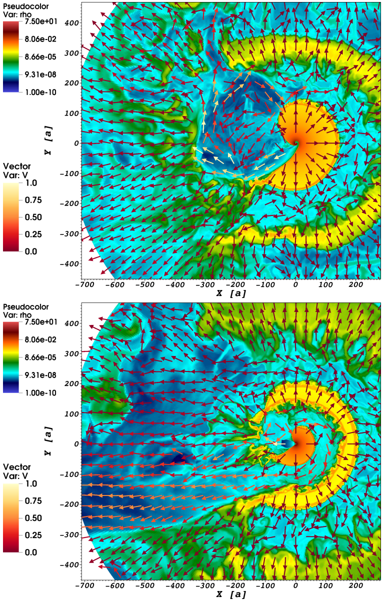

(Barkov & B-R 2018, high *e*)

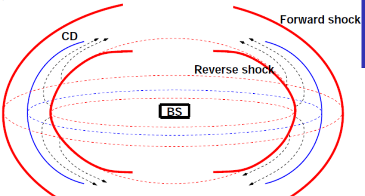

Flow termination. **(B-R & Barkov 2011)**

Mainly X-ray evidence.

(Paredes+2007 -LSI-; Durant+2011 -LS-; Pavlov+2015 -PSRB-, Williams+2015 -1FGL-; Kargaltsev+2021 -HESS-; Albacete-Colombo+2020 -PSRJ- ↓)

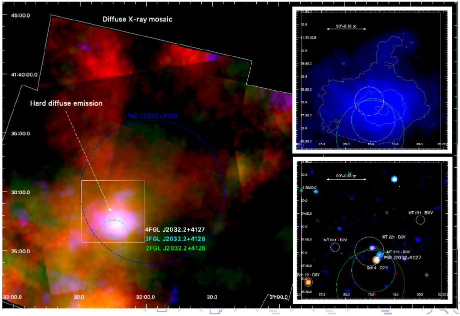

Phenomenological $E_{\rm max}$ in HMGB

- **$E_{\rm max}$ for the most relevant processes ($t_{\rm acc} \sim \eta E/qBc$; $D \sim \chi D_{\rm Bohm}$; $RB \sim$ct?):**
  - **Hillas limit ($e^{\pm}$, p):**
    $E^{\rm H}_{\rm max} \sim 300\, R_{12}\, B_0$ **TeV**
  - **Escape/adiabatic cooling ($e^{\pm}$, p):**
    $E^{\rm dy}_{\rm max} \sim 90\, R_{12}\, B_0\, v_{10}^{-1}\, \eta_1^{-1}$ **TeV**
  - **Diffusion ($e^{\pm}$, p):**
    $E^{\rm diff}_{\rm max} \sim 40\, R_{12}\, B_0\, \eta_1^{-1/2}\, \chi_1^{-1/2}$ **TeV**
  - **Synchrotron ($e^{\pm}$):**
    $E^{\rm sy}_{\rm max} \sim 20\, \eta_1^{-1/2}\, B_0^{-1/2}$**TeV**

(e.g., Rieger et al. 2007; Khangulyan et al. 2008; B-R & Khangulyan 2009; Takahashi et al. 2009 B-R 2012; B-R & Rieger 2012, Derishev & Aharonian 2012)

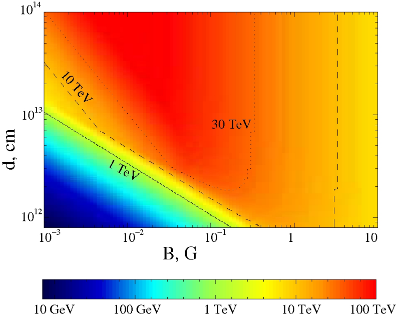

(↑ Khangulyan et al. 2008;↓ Hadasch et al. 2012)

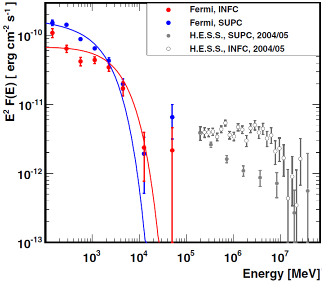

Phenomenological $E_{\rm max}$ in HMGB

- $E_{\rm max}$ **for the most relevant processes ($t_{\rm acc} \sim \eta E/qBc$; $D \sim \chi D_{\rm Bohm}$; $RB \sim$ct?):**
  - **Hillas limit ($e^{\pm}$, p):** $E^{\rm H}_{\rm max} \sim 300\, R_{12}\, B_0$ **TeV**
  - **Escape/adiabatic cooling ($e^{\pm}$, p):** $E^{\rm dy}_{\rm max} \sim 90\, R_{12}\, B_0\, v_{10}^{-1}\, \eta_1^{-1}$ **TeV**
  - **Diffusion ($e^{\pm}$, p):** $E^{\rm diff}_{\rm max} \sim 40\, R_{12}\, B_0\, \eta_1^{-1/2}\, \chi_1^{-1/2}$ **TeV**
  - **Synchrotron ($e^{\pm}$):** $E^{\rm sy}_{\rm max} \sim 20\, \eta_1^{-1/2}\, B_0^{-1/2}$**TeV**

(e.g., Rieger et al. 2007; Khangulyan et al. 2008; B-R & Khangulyan 2009; Takahashi et al. 2009 B-R 2012; B-R & Rieger 2012, Derishev & Aharonian 2012)

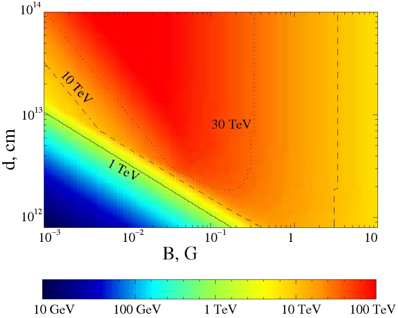

(↑ Khangulyan et al. 2008;↓ Hadasch et al. 2012)

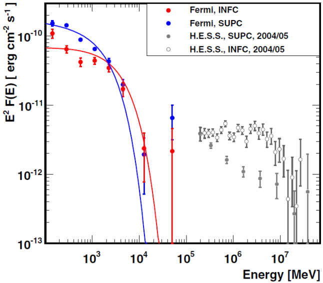

Phenomenological $E_{\rm max}$ in HMGB

- $E_{\rm max}$ **for the most relevant processes ($t_{\rm acc} \sim \eta E/qBc$; $D \sim \chi D_{\rm Bohm}$; $RB \sim$ct?):**
  - **Hillas limit ($e^{\pm}$, p):** $E^{\rm H}_{\rm max} \sim 300\, R_{12}\, B_0$ **TeV**
  - **Escape/adiabatic cooling ($e^{\pm}$, p):** $E^{\rm dy}_{\rm max} \sim 90\, R_{12}\, B_0\, v_{10}^{-1}\, \eta_1^{-1}$ **TeV**
  - **Diffusion ($e^{\pm}$, p):** $E^{\rm diff}_{\rm max} \sim 40\, R_{12}\, B_0\, \eta_1^{-1/2}\, \chi_1^{-1/2}$ **TeV**
  - **Synchrotron ($e^{\pm}$):** $E^{\rm sy}_{\rm max} \sim 20\, \eta_1^{-1/2}\, B_0^{-1/2}$**TeV**

(e.g., Rieger et al. 2007; Khangulyan et al. 2008; B-R & Khangulyan 2009; Takahashi et al. 2009 B-R 2012; B-R & Rieger 2012, Derishev & Aharonian 2012)

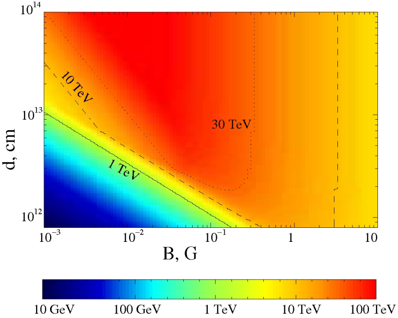

(↑ Khangulyan et al. 2008;↓ Hadasch et al. 2012)

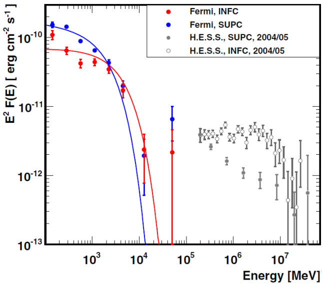

Phenomenological $E_{\rm max}$ in HMGB

- $E_{\rm max}$ **for the most relevant processes ($t_{\rm acc} \sim \eta E/qBc$; $D \sim \chi D_{\rm Bohm}$; $RB \sim$ct?):**
  - **Hillas limit ($e^{\pm}$, p):**
    $E^{\rm H}_{\rm max} \sim 300\, R_{12}\, B_0$ **TeV**
  - **Escape/adiabatic cooling ($e^{\pm}$, p):**
    $E^{\rm dy}_{\rm max} \sim 90\, R_{12}\, B_0\, v_{10}^{-1}\, \eta_1^{-1}$ **TeV**
  - **Diffusion ($e^{\pm}$, p):**
    $E^{\rm diff}_{\rm max} \sim 40\, R_{12}\, B_0\, \eta_1^{-1/2}\, \chi_1^{-1/2}$ **TeV**
  - **Synchrotron ($e^{\pm}$):**
    $E^{\rm sy}_{\rm max} \sim 20\, \eta_1^{-1/2}\, B_0^{-1/2}$**TeV**

(e.g., Rieger et al. 2007; Khangulyan et al. 2008; B-R & Khangulyan 2009; Takahashi et al. 2009 B-R 2012; B-R & Rieger 2012, Derishev & Aharonian 2012)

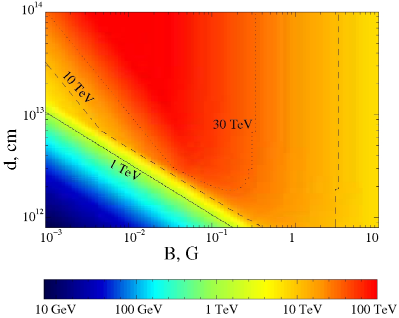

(↑ Khangulyan et al. 2008;↓ Hadasch et al. 2012)

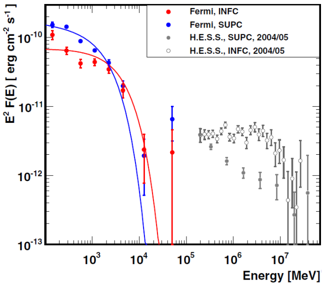

Phenomenological $E_{\rm max}$ in HMGB

- $E_{\rm max}$ **for the most relevant processes ($t_{\rm acc} \sim \eta E/qBc$; $D \sim \chi D_{\rm Bohm}$; $RB \sim$ct?):**
  - **Hillas limit ($e^{\pm}$, p):**
    $E^{\rm H}_{\rm max} \sim 300\, R_{12}\, B_0$ **TeV**
  - **Escape/adiabatic cooling ($e^{\pm}$, p):**
    $E^{\rm dy}_{\rm max} \sim 90\, R_{12}\, B_0\, v_{10}^{-1}\, \eta_1^{-1}$ **TeV**
  - **Diffusion ($e^{\pm}$, p):**
    $E^{\rm diff}_{\rm max} \sim 40\, R_{12}\, B_0\, \eta_1^{-1/2}\, \chi_1^{-1/2}$ **TeV**
  - **Synchrotron ($e^{\pm}$):**
    $E^{\rm sy}_{\rm max} \sim 20\, \eta_1^{-1/2}\, B_0^{-1/2}$**TeV**

(e.g., Rieger et al. 2007; Khangulyan et al. 2008; B-R & Khangulyan 2009; Takahashi et al. 2009 B-R 2012; B-R & Rieger 2012, Derishev & Aharonian 2012)

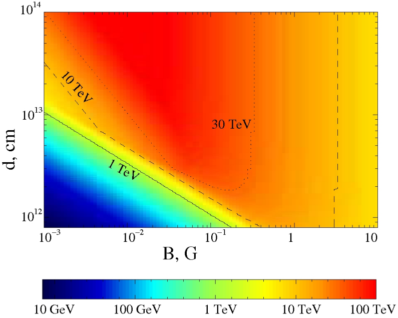

(↑ Khangulyan et al. 2008;↓ Hadasch et al. 2012)

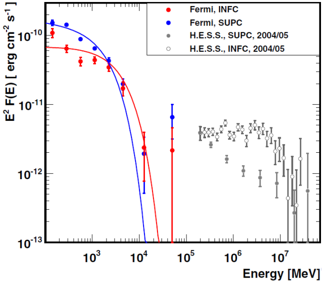

Unshocked pulsar wind acceleration in a HMGB

- **Derishev & Aharonian (2012) showed that the converter mechanism (Derishev et al. 2003; Stern 2003) can operate in compact HMGB via $e^{\pm}$-creation in the unshocked pulsar wind.**
- **The wind loads and slows down while providing a Γ^2-boost to the new $e^{\pm}$, which cool little due to the KN effect (IC) and $B' \approx B/\Gamma$ (sync.) until reaching the shock.** (Derishev & Aharonian 2012)
- **This mechanism may solve several misteries in LS 5039, and perhaps also in LS I +61 303, 1FGL J1018.6−5856...?**

  (Khangulyan et al., B-R et al. 2008; Cerutti et al. 2008; Collmar, W.; B-R 2021...)

  - **Pairs accelerate close to $t_{\rm acc} = E/qBc$, with $\gamma_{\rm peak} \sim \Gamma^2 \sim 10^8$.**
  - **A 1–30 MeV synchrotron (seen) component would arise naturally from postshock synchrotron.**
  - **The (unseen) unshocked pulsar wind SED component would be also smoothed out.**
  - **External cascading effects are closely linked to this process.**

(Derishev & B-R, in prep.)

Unshocked pulsar wind acceleration in a HMGB

- **Derishev & Aharonian (2012) showed that the converter mechanism (Derishev et al. 2003; Stern 2003) can operate in compact HMGB via $e^{\pm}$-creation in the unshocked pulsar wind.**
- **The wind loads and slows down while providing a Γ^2-boost to the new $e^{\pm}$, which cool little due to the KN effect (IC) and $B' \approx B/\Gamma$ (sync.) until reaching the shock.** **(Derishev & Aharonian 2012)**
- **This mechanism may solve several misteries in LS 5039, and perhaps also in LS I +61 303, 1FGL J1018.6−5856...?**

  (Khangulyan et al., B-R et al. 2008; Cerutti et al. 2008; Collmar, W.; B-R 2021...)

  - **Pairs accelerate close to $t_{\rm acc} = E/qBc$, with $\gamma_{\rm peak} \sim \Gamma^2 \sim 10^8$.**
  - **A 1–30 MeV synchrotron (seen) component would arise naturally from postshock synchrotron.**
  - **The (unseen) unshocked pulsar wind SED component would be also smoothed out.**
  - **External cascading effects are closely linked to this process.**

(Derishev & B-R, in prep.)

Unshocked pulsar wind acceleration in a HMGB

- **Derishev & Aharonian (2012) showed that the converter mechanism (Derishev et al. 2003; Stern 2003) can operate in compact HMGB via $e^{\pm}$-creation in the unshocked pulsar wind.**
- **The wind loads and slows down while providing a Γ^2-boost to the new $e^{\pm}$, which cool little due to the KN effect (IC) and $B' \approx B/\Gamma$ (sync.) until reaching the shock.** (Derishev & Aharonian 2012)
- **This mechanism may solve several misteries in LS 5039, and perhaps also in LS I +61 303, 1FGL J1018.6−5856...?**

(Khangulyan et al., B-R et al. 2008; Cerutti et al. 2008; Collmar, W.; B-R 2021...)

  - Pairs accelerate close to $t_{\rm acc} = E/qBc$, with $\gamma_{\rm peak} \sim \Gamma^2 \sim 10^8$.
  - A 1–30 MeV synchrotron (seen) component would arise naturally from postshock synchrotron.
  - The (unseen) unshocked pulsar wind SED component would be also smoothed out.
  - External cascading effects are closely linked to this process.

(Derishev & B-R, in prep.)

Unshocked pulsar wind acceleration in a HMGB

- **Derishev & Aharonian (2012) showed that the converter mechanism (Derishev et al. 2003; Stern 2003) can operate in compact HMGB via $e^{\pm}$-creation in the unshocked pulsar wind.**
- **The wind loads and slows down while providing a Γ^2-boost to the new $e^{\pm}$, which cool little due to the KN effect (IC) and $B' \approx B/\Gamma$ (sync.) until reaching the shock.** **(Derishev & Aharonian 2012)**
- **This mechanism may solve several misteries in LS 5039, and perhaps also in LS I +61 303, 1FGL J1018.6−5856...?**

(Khangulyan et al., B-R et al. 2008; Cerutti et al. 2008; Collmar, W.; B-R 2021...)

  - **Pairs accelerate close to $t_{\rm acc} = E/qBc$, with $\gamma_{\rm peak} \sim \Gamma^2 \sim 10^8$.**
  - A 1–30 MeV synchrotron (seen) component would arise naturally from postshock synchrotron.
  - The (unseen) unshocked pulsar wind SED component would be also smoothed out.
  - External cascading effects are closely linked to this process.

(Derishev & B-R, in prep.)

Unshocked pulsar wind acceleration in a HMGB

- Derishev & Aharonian (2012) showed that the converter mechanism (Derishev et al. 2003; Stern 2003) can operate in compact HMGB via $e^{\pm}$-creation in the unshocked pulsar wind.
- The wind loads and slows down while providing a Γ^2-boost to the new $e^{\pm}$, which cool little due to the KN effect (IC) and $B' \approx B/\Gamma$ (sync.) until reaching the shock. (Derishev & Aharonian 2012)
- This mechanism may solve several misteries in LS 5039, and perhaps also in LS I +61 303, 1FGL J1018.6$-$5856...?

(Khangulyan et al., B-R et al. 2008; Cerutti et al. 2008; Collmar, W.; B-R 2021...)

  - Pairs accelerate close to $t_{\rm acc} = E/qBc$, with $\gamma_{\rm peak} \sim \Gamma^2 \sim 10^8$.
  - A 1–30 MeV synchrotron (seen) component would arise naturally from postshock synchrotron.
  - The (unseen) unshocked pulsar wind SED component would be also smoothed out.
  - External cascading effects are closely linked to this process.

(Derishev & B-R, in prep.)

Unshocked pulsar wind acceleration in a HMGB

- **Derishev & Aharonian (2012) showed that the converter mechanism (Derishev et al. 2003; Stern 2003) can operate in compact HMGB via $e^{\pm}$-creation in the unshocked pulsar wind.**
- **The wind loads and slows down while providing a Γ^2-boost to the new $e^{\pm}$, which cool little due to the KN effect (IC) and $B' \approx B/\Gamma$ (sync.) until reaching the shock.** (Derishev & Aharonian 2012)
- **This mechanism may solve several misteries in LS 5039, and perhaps also in LS I +61 303, 1FGL J1018.6$-$5856...?**

(Khangulyan et al., B-R et al. 2008; Cerutti et al. 2008; Collmar, W.; B-R 2021...)

  - **Pairs accelerate close to $t_{\rm acc} = E/qBc$, with $\gamma_{\rm peak} \sim \Gamma^2 \sim 10^8$.**
  - **A 1–30 MeV synchrotron (seen) component would arise naturally from postshock synchrotron.**
  - **The (unseen) unshocked pulsar wind SED component would be also smoothed out.**
  - **External cascading effects are closely linked to this process.**

(Derishev & B-R, in prep.)

Unshocked pulsar wind acceleration in a HMGB

- **Derishev & Aharonian (2012) showed that the converter mechanism (Derishev et al. 2003; Stern 2003) can operate in compact HMGB via $e^{\pm}$-creation in the unshocked pulsar wind.**
- **The wind loads and slows down while providing a Γ^2-boost to the new $e^{\pm}$, which cool little due to the KN effect (IC) and $B' \approx B/\Gamma$ (sync.) until reaching the shock.** (Derishev & Aharonian 2012)
- **This mechanism may solve several misteries in LS 5039, and perhaps also in LS I +61 303, 1FGL J1018.6−5856...?**

  (Khangulyan et al., B-R et al. 2008; Cerutti et al. 2008; Collmar, W.; B-R 2021...)

  - **Pairs accelerate close to $t_{\rm acc} = E/qBc$, with $\gamma_{\rm peak} \sim \Gamma^2 \sim 10^8$.**
  - **A 1–30 MeV synchrotron (seen) component would arise naturally from postshock synchrotron.**
  - **The (unseen) unshocked pulsar wind SED component would be also smoothed out.**
  - **External cascading effects are closely linked to this process.**

(Derishev & B-R, in prep.)

Outline

Final remarks

- **HMGB are perfect sites for multi-TeV particle acceleration and radiation.**
- **However, leptonic and hadronic CR injection from the system may be inefficient due to adiabatic losses.**
- **On the other hand, large-scale outflow-medium interactions might be a suitable site for PeV CR production (large scale X-rays).**
- **Finally, as LS 5039, LS I 61 040, 1FGL J1018.6$-$5856, 4FGL J1405.1-6119... are known within $\sim 1/4$ of the disk.**
- **The total power of the HMGB population may be $\gtrsim 10^{38}$ erg $^{-1}$.**

Final remarks

- **HMGB are perfect sites for multi-TeV particle acceleration and radiation.**
- **However, leptonic and hadronic CR injection from the system may be inefficient due to adiabatic losses.**
- **On the other hand, large-scale outflow-medium interactions might be a suitable site for PeV CR production (large scale X-rays).**
- **Finally, as LS 5039, LS I 61 040, 1FGL J1018.6−5856, 4FGL J1405.1-6119... are known within $\sim 1/4$ of the disk.**
- **The total power of the HMGB population may be $\gtrsim 10^{38}$ erg $^{-1}$.**

Final remarks

- **HMGB are perfect sites for multi-TeV particle acceleration and radiation.**
- **However, leptonic and hadronic CR injection from the system may be inefficient due to adiabatic losses.**
- **On the other hand, large-scale outflow-medium interactions might be a suitable site for PeV CR production (large scale X-rays).**
- **Finally, as LS 5039, LS I 61 040, 1FGL J1018.6$-$5856, 4FGL J1405.1-6119... are known within $\sim 1/4$ of the disk.**
- **The total power of the HMGB population may be $\gtrsim 10^{38}$ erg $^{-1}$.**

Final remarks

- **HMGB are perfect sites for multi-TeV particle acceleration and radiation.**
- **However, leptonic and hadronic CR injection from the system may be inefficient due to adiabatic losses.**
- **On the other hand, large-scale outflow-medium interactions might be a suitable site for PeV CR production (large scale X-rays).**
- **Finally, as LS 5039, LS I 61 040, 1FGL J1018.6$-$5856, 4FGL J1405.1-6119... are known within $\sim 1/4$ of the disk.**
- **The total power of the HMGB population may be $\gtrsim 10^{38}$ erg $^{-1}$.**

Final remarks

- **HMGB are perfect sites for multi-TeV particle acceleration and radiation.**
- **However, leptonic and hadronic CR injection from the system may be inefficient due to adiabatic losses.**
- **On the other hand, large-scale outflow-medium interactions might be a suitable site for PeV CR production (large scale X-rays).**
- **Finally, as LS 5039, LS I 61 040, 1FGL J1018.6$-$5856, 4FGL J1405.1-6119... are known within $\sim 1/4$ of the disk.**
- **The total power of the HMGB population may be $\gtrsim 10^{38}$ erg $^{-1}$.**